Chapter 11
Spintronics

11.1 Introduction

The materials that have been considered thus far in the book are 'classical,' in the sense that their electromagnetic properties are easily stated as parameters that can be easily measured in the laboratory, or can be computed and understood using 'classical' physics. This is true whether the materials are 'structural' or 'biological'. Furthermore, we have shown that materials of these two classes can be characterized using the same classical electromagnetic models.

In order to expand our understanding and application of electromagnetic models to materials, we must consider cases in which the above statements do not hold, and one must resort to more sophisticated physical models that incorporate quantum mechanical principles just to understand the interaction of the electromagnetic field with the material. There are a number of common and novel materials in which this is true. For example, the interaction of an electromagnetic field in a microwave solid-state maser can only be understood through the application of the quantum theory of paramagnetism and electron spin dynamics [117]. Another well-known example is nuclear magnetic resonance (NMR), in which the spin of the proton in the nucleus of atoms provides the interaction that leads to magnetic resonance imaging (MRI).

11.2 Paramagnetic Spin Dynamics and the Spin Hamiltonian

In order to fully understand the possibilities of using paramagnetic phenomena to detect lesions noninvasively, we must review a bit of electron-spin physics. Our interest is in the dynamic response of spins to time-varying fields. These fields are

either applied electromagnetic fields or fluctuating fields due to random vibrations of the crystalline surroundings of the spin system.[1]

The system of equations used to describe spin dynamics is derived from Schrödinger's wave equation of quantum mechanics, and is given by

$$\frac{d\rho_{mn}}{dt} = \frac{j}{\hbar} \sum_{k} (\rho_{mk}\mathcal{H}_{kn} - \mathcal{H}_{mk}\rho_{kn}) + \sum_{pq} R_{mn,pq} \left(\rho_{pq} - \rho_{pq}^{(T)} \right) , \qquad (11.1)$$

where ρ_{mn} is the density matrix connecting energy states u_m and u_n of the unperturbed system, $R_{mn,pq}$ are real numbers that account for spin-lattice relaxation, and the superscript, T, denotes the thermal equilibrium density matrix. $\mathcal{H}_{jk} = \mathcal{H}_{0jk} + \mathcal{H}_{1jk}(t)$, where $\mathcal{H}_{0jk}$ is the unperturbed, time-independent spin-Hamiltonian associated with the crystalline field, and $\mathcal{H}_{1jk}(t) = gh\beta \left[\mathbf{H}(t) \cdot \mathbf{S} \right]_{jk}$ is the time-dependent perturbation. Here g is a constant, $h\beta$ the Bohr magneton, h Planck's constant, $\hbar = h/2\pi$, $\mathbf{H}(t)$ the time-dependent (rf) magnetic field, and $\mathbf{S} = S_x\mathbf{a}_x + S_y\mathbf{a}_y + S_z\mathbf{a}_z$ is the vector spin operator.

Because $\{u_m\}$ is an orthonormal system of eigenstates of $\mathcal{H}_0$, it follows immediately that $\mathcal{H}_{0mm} = E_m$, and all off-diagonal elements of $\mathcal{H}_{0mn}$ vanish. Furthermore, in order to get a linear (i.e., first-order in $\mathbf{H}(t)$) response for the overall system, we must set the diagonal terms of (11.1) to their thermal equilibrium values, $\rho_{mn}(t) = \rho_{mn}^{(T)}$, and solve the off-diagonal terms to first-order in $\mathbf{H}(t)$:

$$\frac{d\rho_{mn}}{dt} = \left(j\omega_{0mn} - \frac{1}{\tau_{mn}} \right) \rho_{mn} + \frac{j}{\hbar} \left(\rho_{mm}^{(T)} - \rho_{nn}^{(T)} \right) \mathcal{H}_{1mn}(t) , \qquad (11.2)$$

where $\omega_{0mn} = \dfrac{E_n - E_m}{\hbar}$, and the relaxation times, τ_{mn}, replace the $R_{mn,pq}$ of (11.1).

For a sinusoidally time-varying field, we have $\mathcal{H}_{1mn}(t) = \dfrac{g\beta h}{2} \left(\mathbf{H}e^{j\omega t} + \mathbf{H}^* e^{-j\omega t} \right) \cdot \mathbf{S}_{mn}$. If we assume solutions of (11.2) of the form $\rho_{mn} = A_{mn}e^{j\omega t} + B_{mn}e^{-j\omega t}$, then the coefficients of the positive-frequency terms, A_{mn}, and negative-frequency terms, B_{mn}, are given by

$$A_{mn} = \frac{(j/\hbar) \left(\rho_{mm}^{(T)} - \rho_{nn}^{(T)} \right) \tau_{mn} g\beta h/2}{1 - j(-\omega + \omega_{0mn}) \tau_{mn}} \mathbf{S}_{mn} \cdot \mathbf{H}$$

$$B_{mn} = \frac{(j/\hbar) \left(\rho_{mm}^{(T)} - \rho_{nn}^{(T)} \right) \tau_{mn} g\beta h/2}{1 - j(\omega + \omega_{0mn}) \tau_{mn}} \mathbf{S}_{mn} \cdot \mathbf{H} . \qquad (11.3)$$

---

[1]This discussion follows [96], which deals with spin dynamics in the crystalline field of a solid-state maser. Later we will discuss the changes that occur when the spin system is in a noncrystalline environment, such as biological tissue.

The magnetic dipole-moment operator for each spin is $g\beta h\mathbf{S}$, which means that the average dipole-moment for each spin is $\mathbf{m} = \mathrm{Tr}\,[\rho g\beta h\mathbf{S}]$, where Tr is the trace of an operator (sum of the diagonal elements of its matrix representation). The macroscopic dipole-moment per unit volume, $\mathbf{M}$, is obtained by multiplying $\mathbf{m}$ by the number density, N, of spins. Upon evaluating the trace, we find

$$
\mathbf{M} = \gamma^2 \sum_{j<k} \mathbf{S}_{kj}\mathbf{S}_{jk}\left(N_j^{(T)} - N_k^{(T)}\right)
$$

$$
\tau_{jk}\left[\left(\frac{j/\hbar}{1 - j(\omega_{0jk} - \omega)\tau_{jk}} - \frac{j/\hbar}{1 + j(\omega_{0jk} + \omega)\tau_{jk}}\right)\mathbf{H}e^{j\omega t}\right.
$$

$$
\left. + \left(\frac{-j/\hbar}{1 + j(\omega_{0jk} - \omega)\tau_{jk}} - \frac{-j/\hbar}{1 - j(\omega_{0jk} + \omega)\tau_{jk}}\right)\mathbf{H}^*e^{-j\omega t}\right] , \quad (11.4)
$$

where we have discarded the time-independent static dipole terms, $\mathbf{S}_{mm}\rho_{mm}^{(T)}$, and have set $\gamma^2 = g^2 h^2 \beta^2$. $N_j^{(T)}$ is the number of spins per-unit-volume occupying the jth energy level when the system is in thermal equilibrium at temperature T. If N is the total number of spins (or systems) in the crystal, then $N_j^{(T)} = \dfrac{N}{Z}\exp(-E_j/kT)$, where $Z = \sum_{j=1}^{J}\exp(-E_j/kT)$ and J is the total number of energy states. Thus, at thermal equilibrium (at positive temperatures), the lower energy states are more densely populated than the higher energy states.

The absorption spectrum, $A(\omega)$, is given by μ_0 times the imaginary part of the generalized magnetic susceptibility, which is the coefficient of $\mathbf{H}e^{j\omega t}$ in (11.4). In the vicinity of the resonant frequency, ω_{0jk}, the absorption spectrum is

$$
A(\omega) \approx \mu_0 \frac{\gamma^2}{2}\sum_{j<k}|S_{kj}|^2\left(N_j^{(T)} - N_k^{(T)}\right)\frac{\tau_{jk}/\hbar}{1 + (\omega_{0jk} - \omega)^2\tau_{jk}^2}
$$

$$
= \mu_0\frac{\gamma^2}{2}\frac{N}{Z}\sum_{j<k}|S_{kj}|^2\left(e^{-E_j/kT} - e^{-E_k/kT}\right)\frac{\tau_{jk}/\hbar}{1 + (\omega_{0jk} - \omega)^2\tau_{jk}^2} . \quad (11.5)
$$

This spectrum consists of 'lorentzian' curves (resonant curves) centered at the frequencies ω_{0jk}, with line-width $1/\tau_{jk}$. The peak of each resonance is proportional to τ_{jk}, and this gives us the familiar trade-off between bandwidth and magnitude of absorption (or magnitude of gain). The term $N_j^{(T)} - N_k^{(T)}$ yields the population difference per unit volume of the jth and kth energy levels when the system is in thermal equilibrium at temperature T. This population difference will be small if the energy differential, $E_k - E_j$, is small compared to the thermal energy, kT, as is the usual case for paramagnetic spin systems at normal temperatures. In addition to τ_{jk}, an important parameter is the 'line-strength', $|S_{kj}|^2$, or the transition matrix element connecting the jth and kth states. It determines the ease with which pump power is absorbed by the spins, or it determines the gain at signal frequencies.

11.2.1 *Application to* Fe^{3+} : TiO_2

The five unpaired electrons in Fe^{3+} are each in the 3d state, meaning that the ion is in an S-state, with a spin, $S = 5/2$. The total number of spin-states, therefore, is $N_s = 2S + 1 = 6$. The spin-Hamiltonian, $\mathscr{H}_0$, for the Fe^{3+} : TiO_2 complex is [96]

$$\mathscr{H}_0 = g\beta \mathbf{H}_0 \cdot \mathbf{S} + D\left(S_z^2 - 35/12\right) + E\left(S_x^2 - S_y^2\right) + (a/6)\left(S_x^4 + S_y^4 + S_z^4 - 707/16\right)$$

$$+ (7/36)F\left(S_z^4 - (95/14)S_z^2 + 81/16\right) , \tag{11.6}$$

where the nominal values of the derived constants are $g = 2.0$, $D = 20.35\,GHz$, $E = 2.21\,GHz$, $a = 1.1\,GHz$, $F = -0.5\,GHz$, and H_0 is the dc magnetic field. S_x, S_y, and S_z are 6×6 Pauli spin-matrices. This Hamiltonian gives us frequency directly, rather than energy. The D term has axial symmetry (about the z-axis), and corresponds to the ion having an electric quadrupole moment, that is acted upon by the crystalline electric fields. The E term represents and additional nonaxially symmetric anisotropy in the xy plane, and corresponds to the ion's possessing an electric moment of higher order than quadrupolar. These are the main terms, as the size of D and E would suggest; the remaining terms are due to the fact that $S > 2$ and that the crystal symmetry is complicated. Clearly, these latter terms are less important, but must be included for completeness.

The eigenvalue equation that determines the unperturbed energy levels (or frequencies in this case) is

$$\mathscr{H}_0 u = E u , \tag{11.7}$$

and when this equation is solved as a function of $\mathbf{H}_0 = H\mathbf{a}_z$, we get the six curves shown in Fig. 11.1. The zero-field energies occur in pairs (Kramers' doublets), as is typical of a system with an odd number of electrons in an electric field (the crystalline field).

Consider the system at $H = 1.78$ kilogauss; the eigenvalues of $\mathscr{H}_0$ are

$$\begin{aligned} &E_1 = -58.20 \times 10^9 h \quad E_2 = -54.15 \times 10^9 h \quad E_3 = -19.60 \times 10^9 h \\ &E_4 = -5.64 \times 10^9 h \quad E_5 = 56.14 \times 10^9 h \quad E_6 = 81.05 \times 10^9 h \end{aligned} , \tag{11.8}$$

from which we derive the resonant frequencies (in GHz)

$$\begin{aligned} &\omega_{012} = 4.05 \quad \omega_{023} = 34.55 \quad \omega_{034} = 13.96 \quad \omega_{045} = 61.78 \quad \omega_{056} = 24.91 \\ &\omega_{013} = 38.60 \quad \omega_{024} = 48.51 \quad \omega_{035} = 75.74 \quad \omega_{046} = 86.69 \\ &\omega_{014} = 52.56 \quad \omega_{025} = 110.29 \quad \omega_{036} = 100.65 \\ &\omega_{015} = 114.34 \quad \omega_{026} = 135.20 \\ &\omega_{016} = 139.25 \end{aligned} , \tag{11.9}$$

Fig. 11.1 Six-fold energy levels (in frequency units) for Fe^{3+} : TiO_2, as a function of the z-directed magnetic field, H
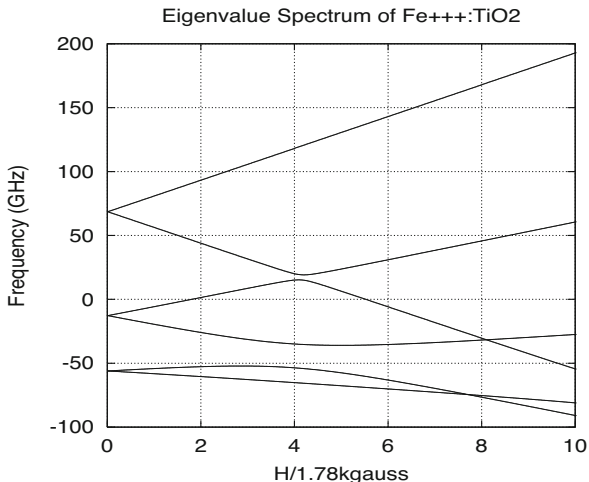
and the transition-matrix elements

$$
\begin{array}{lllll}
S_{x12} = 0.8 & S_{x23} = 0 & S_{x34} = -0.69 & S_{x45} = 0 & S_{x56} = 0 \\
S_{x13} = 1.66 & S_{x24} = -1.50 & S_{x35} = 1.08 & S_{x46} = 1.10 & \\
S_{x14} = 0 & S_{x25} = -0.31 & S_{x36} = 0 & & \\
S_{x15} = 0 & S_{x26} = 0 & & & \\
S_{x16} = 0 & & & &
\end{array}
$$

$$
\begin{array}{lllll}
S_{y12} = -j0.8 & S_{y23} = 0 & S_{y34} = -j0.53 & S_{y45} = 0 & S_{y56} = 0 \\
S_{y13} = -j1.66 & S_{y24} = -j1.02 & S_{y35} = -j1.08 & S_{y46} = j1.10 & \\
S_{y14} = 0 & S_{y25} = j0.31 & S_{y36} = 0 & & \\
S_{y15} = 0 & S_{y26} = 0 & & & \\
S_{y16} = j0.19 & & & &
\end{array}
$$

$$
\begin{array}{lllll}
S_{z12} = 0 & S_{z23} = 0.54 & S_{z34} = 0 & S_{z45} = 0 & S_{z56} = 0 \\
S_{z13} = 0 & S_{z24} = 0 & S_{z35} = 0 & S_{z46} = 0 & \\
S_{z14} = 0.33 & S_{z25} = 0 & S_{z36} = 0 & & \\
S_{z15} = 0 & S_{z26} = 0 & & & \\
S_{z16} = 0 & & & &
\end{array}
$$

$$(11.10)$$

From these results we can conclude, for example, that a transition between states 1 and 2 (4.05 GHz) has a 'strength' of $(0.8)^2$ for either x- or y-polarized radiation at that frequency, but cannot occur for z-polarized radiation. Similarly, we can answer the question of pump transitions. There are only two possible pump transitions, the 1–4 transition at 52.56 GHz and the 2–3 transition at 34.55 GHz, if one uses z-polarized pump radiation. If, however, we wish to amplify a signal at 4.05 GHz

Fig. 11.2 Absorption spectrum in vicinity of 4.05 GHz, with $\tau_{12} = 5.305 \times 10^{-9}$ s. The half-power width is 60 MHz
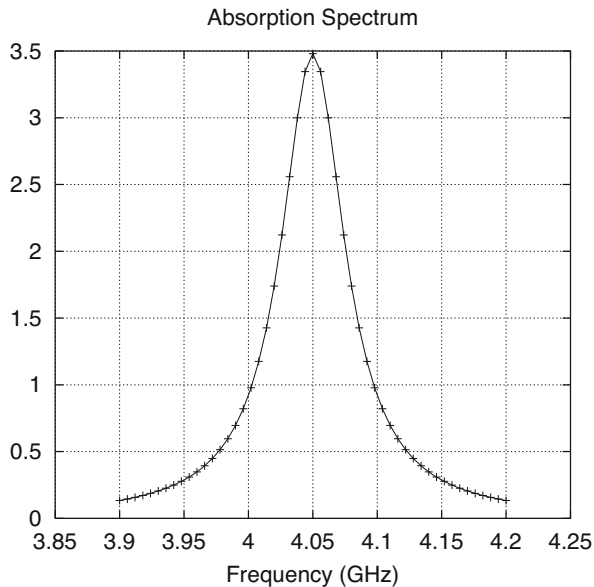
(1–2 transition) we must pump between the first level and the third or higher level. Hence, we consider pumping only the 1–3 or 1–4 transition if we wish to remain below 100 GHz. The only possible 1–4 transition uses z-polarized radiation and has a strength of $(0.33)^2$. If we pump at 38.60 GHz (the 1–3 transition) we may use x- or y-polarized radiation (or both, as in circular polarization) and improve the absorption strength to $(1.66)^2$.

The width of the absorption curve for the 1–2 (4.05 GHz) transition of $Fe^{3+} : TiO_2$ is 60 MHz. Hence, the spin-lattice relaxation (or simply the *transverse relaxation*) time for the off-diagonal element, ρ_{12}, is $\tau_{12} = 1/2\pi \times 30 \times 10^6 = 5.305 \times 10^{-9}$ s. Figure 11.2 shows the absorption spectrum in the vicinity of 4.05 GHz with this value of τ_{12}.

This example illustrates the utility of the eigenstates in determining the frequency response of a maser. It relies, as we have noted, on knowledge of the crystalline-field environment of the iron ion. It is this information that is lacking when we consider electron-paramagnetic spin systems in biological tissue, and is the basis for one of our research proposals.

11.2.2 Ho^{++} : CaF$_2$

Holmium is a type 4f rare earth, which means that the divalent Holmium ion has its unpaired electrons in the 4f shell where they are effectively screened from their crystalline surroundings by electrons in the outer shells. Therefore, as a reasonable

approximation to the effective spin-Hamiltonian we may discard any terms that represent the crystalline field. We must, however, include the spin-spin interaction between the unpaired electrons and the nucleus because these electrons are relatively close to the nucleus. Thus, we use the following spin-Hamiltonian

$$\mathcal{H}_0 = g\beta \mathbf{H}_0 \cdot \mathbf{S} + A\mathbf{I} \cdot \mathbf{S} \,, \tag{11.11}$$

where $g = 5.91$, $\beta = 0.0014$ GHz/gauss, $A = 3.924$ GHz, $\mathbf{S}$ is the electron spin operator, with effective spin 1/2, and $\mathbf{I}$ is the nuclear spin operator with spin 7/2.

Because we are dealing with a system of two particles (electron plus nucleus) we cannot simply form matrix products in order to evaluate $\mathcal{H}_0$, but must use the direct product of the appropriate Pauli spin matrices of $\mathbf{I}$ and $\mathbf{S}$. Because there are two possible electron spin-states ("spin up" and "spin down" relative to, say, the axis of $\mathbf{H}_0$) and $2 \times 7/2 + 1 = 8$ possible spin states of the nucleus, we have a composite system of 16 possible states. This means that the combined spin-Hamiltonian, (11.11), will be represented by a 16×16 matrix. When this matrix is written out, and its eigenvalues determined as a function of magnetic field, we get the plot of Fig. 11.3.

A comparison of Figs. 11.1 and 11.3 shows that Ho^{++} has a much more uniform variation of energy (and, hence, resonant frequency) with H than does Fe^{3+}. This follows, as has been mentioned before, because the unpaired electrons in Ho^{++} are screened from the crystalline field, whereas those of Fe^{3+} are not. Hence, Ho^{2+}
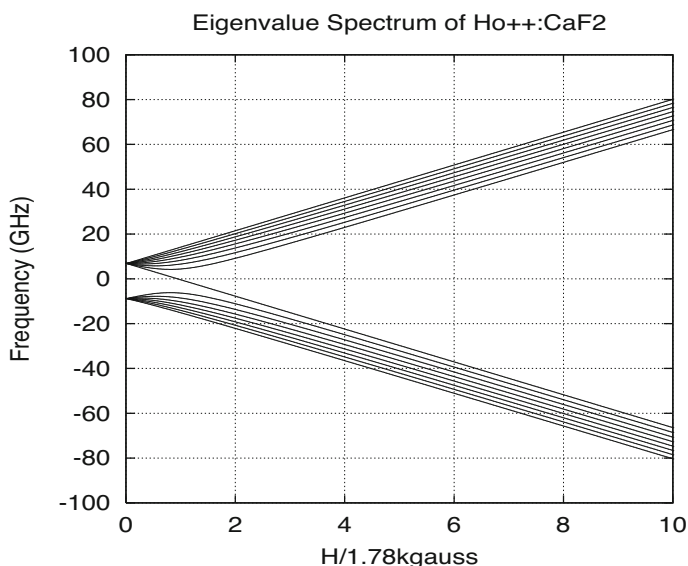

Fig. 11.3 Sixteen-fold energy levels (in frequency units) for Ho^{++} : CaF_2, as a function of the z-directed magnetic field, H

behaves, for H greater than 3 kilogauss, as a free spin in an external magnetic field. We would expect this same qualitative behavior for many of the 4f rare earths, no matter what the crystal lattice is. This suggests that if we use 4f rare-earth spin-systems, it may not be necessary to know anything about the electric-field environment of the biological tissue.

11.3 Superparamagnetic Iron Oxide

This is what started this discussion of paramagnetic spin-systems. Iron oxide, whether it is $\gamma - Fe_2O_3$, called 'maghemite,' or, perhaps magnetite, Fe_3O_4 ([95] is not clear on this), is ferromagnetic. Because of the small size of the particles (~ 10 nm), their ferromagnetic properties manifest themselves in a single domain, and such single domain particles can behave magnetically in a manner analogous to the paramagnetism of moment-bearing atoms [16]. The main distinction is that the moment of the particle may be 10^5 times the atomic moment, because of the 10^5 atoms ferromagnetically coupled by exchange forces within the single domain.[2,3]

Two Spins We'll make a simple quantum-mechanical calculation of a system of two electrons coupled through the exchange interaction in a static magnetic field, $\mathbf{H}_0$. The Hamiltonian is

$$\mathcal{H} = -g\beta \mathbf{H}_0 \cdot \left(\mathbf{S}^{(1)} + \mathbf{S}^{(2)} \right) - 2J_{exch} \mathbf{S}^{(1)} \cdot \mathbf{S}^{(2)} , \qquad (11.12)$$

where $g\beta = g \times 0.0014$ GHz/gauss $= 2.8$ GHz/kgauss, if we take $g = 2$. J_{exch} is the exchange energy, with a nominal value of 2.1×10^{-21} J. Dividing by Plancks constant, h, gives us the result in frequency units: $J_{exch}/h = 2.1 \times 10^{-21}/6.626 \times 10^{-34} = 3169.3$ GHz. Hence, the normalized Hamiltonian for the system becomes

$$\mathcal{H} = -2.8\mathbf{H}_0 \cdot \left(\mathbf{S}^{(1)} + \mathbf{S}^{(2)} \right) - 6338.7 \mathbf{S}^{(1)} \cdot \mathbf{S}^{(2)}$$
$$= -2.8 H_0 \left(S_z^{(1)} + S_z^{(2)} \right) - 6338.7 \mathbf{S}^{(1)} \cdot \mathbf{S}^{(2)} , \qquad (11.13)$$

where we assume that the static field is along the z-direction.

---

[2]Additional References on Superparamagnetic and Ferromagnetic Effects: [6, 23, 25, 49, 67, 75, 76, 116, 119, 124, 136].

[3]By a 'single domain particle,' we mean a particle that is in a state of uniform magnetization at any magnetic field[16].

The Pauli spin-matrices for a single electron in a z-directed magnetic field are

$$s_x = \frac{1}{2}\begin{bmatrix} 0 & 1 \\ 1 & 0 \end{bmatrix} \quad s_y = \frac{1}{2}\begin{bmatrix} 0 & -j \\ j & 0 \end{bmatrix} \quad s_z = \frac{1}{2}\begin{bmatrix} 1 & 0 \\ 0 & -1 \end{bmatrix}, \tag{11.14}$$

and the eigenstates of s_z are $\begin{bmatrix} 1 \\ 0 \end{bmatrix}$, $\begin{bmatrix} 0 \\ 1 \end{bmatrix}$, with the first one corresponding to 'spin up' (parallel to the magnetic field), and the second to 'spin down' (antiparallel to the magnetic field).

Since we have two coupled spins, we must work in the four-dimensional direct-product space of the operators of (11.14):

$$S_x^{(1)} S_x^{(2)} = \frac{1}{4}\begin{bmatrix} 0 & 0 & 0 & 1 \\ 0 & 0 & 1 & 0 \\ 0 & 1 & 0 & 0 \\ 1 & 0 & 0 & 0 \end{bmatrix}$$

$$S_y^{(1)} S_y^{(2)} = \frac{1}{4}\begin{bmatrix} 0 & 0 & 0 & -1 \\ 0 & 0 & 1 & 0 \\ 0 & 1 & 0 & 0 \\ -1 & 0 & 0 & 0 \end{bmatrix}$$

$$S_z^{(1)} S_z^{(2)} = \frac{1}{4}\begin{bmatrix} 1 & 0 & 0 & 0 \\ 0 & -1 & 0 & 0 \\ 0 & 0 & -1 & 0 \\ 0 & 0 & 0 & 1 \end{bmatrix}$$

$$\mathbf{S}^{(1)} \cdot \mathbf{S}^{(2)} = S_x^{(1)} S_x^{(2)} + S_y^{(1)} S_y^{(2)} + S_z^{(1)} S_z^{(2)}$$

$$= \frac{1}{4}\begin{bmatrix} 1 & 0 & 0 & 0 \\ 0 & -1 & 2 & 0 \\ 0 & 2 & -1 & 0 \\ 0 & 0 & 0 & 1 \end{bmatrix}. \tag{11.15}$$

The four-dimensional representations of S_x, S_y, S_z are obtained by taking the left- and right-direct products of the single-electron Pauli spin-matrices, (11.14), with the two-dimensional identity matrix. The results are

$$
S_x^{(1)} = \frac{1}{2}
\begin{bmatrix}
0 & 0 & 1 & 0 \\
0 & 0 & 0 & 1 \\
1 & 0 & 0 & 0 \\
0 & 1 & 0 & 0
\end{bmatrix}
\quad
S_y^{(1)} = \frac{1}{2}
\begin{bmatrix}
0 & 0 & -j & 0 \\
0 & 0 & 0 & -j \\
j & 0 & 0 & 0 \\
0 & j & 0 & 0
\end{bmatrix}
\quad
S_z^{(1)} = \frac{1}{2}
\begin{bmatrix}
1 & 0 & 0 & 0 \\
0 & 1 & 0 & 0 \\
0 & 0 & -1 & 0 \\
0 & 0 & 0 & -1
\end{bmatrix}
$$

$$
S_x^{(2)} = \frac{1}{2}
\begin{bmatrix}
0 & 1 & 0 & 0 \\
1 & 0 & 0 & 0 \\
0 & 0 & 0 & 1 \\
0 & 0 & 1 & 0
\end{bmatrix}
\quad
S_y^{(2)} = \frac{1}{2}
\begin{bmatrix}
0 & -j & 0 & 0 \\
j & 0 & 0 & 0 \\
0 & 0 & 0 & -j \\
0 & 0 & j & 0
\end{bmatrix}
\quad
S_z^{(2)} = \frac{1}{2}
\begin{bmatrix}
1 & 0 & 0 & 0 \\
0 & -1 & 0 & 0 \\
0 & 0 & 1 & 0 \\
0 & 0 & 0 & -1
\end{bmatrix}
$$

$$(11.16)$$

for the two particles. Note that these two-particle spin matrices satisfy the general commutation relations $\left[S_x^{(p)}, S_y^{(q)} \right] = j\delta_{pq} S_z^{(p)}$. Note further that the product of these matrices gives the same results that we obtained independently in (11.15).

The eigenvectors of the matrix, $S_z^{(1)} + S_z^{(2)}$, in (11.16) are the direct products of the eigenstates of the two-dimensional Pauli spin-matrix, s_z:

$$
\begin{bmatrix} 1 \\ 0 \\ 0 \\ 0 \end{bmatrix}
\begin{bmatrix} 0 \\ 1 \\ 0 \\ 0 \end{bmatrix}
\begin{bmatrix} 0 \\ 0 \\ 1 \\ 0 \end{bmatrix}
\begin{bmatrix} 0 \\ 0 \\ 0 \\ 1 \end{bmatrix}
\tag{11.17}
$$

The first eigenvector in (11.17) corresponds to both spins in the 'up' position (both parallel to the magnetic field), the second to 'spin up; spin down,' the third to 'spin down; spin up,' and the fourth to 'spin down; spin down.'

With this background, we can now write down the matrix representation of the normalized spin-Hamiltonian (11.13):

$$
\mathscr{H} =
\begin{bmatrix}
-2.8H_0 - 1584.7 & 0 & 0 & 0 \\
0 & 1584.7 & -3169.4 & 0 \\
0 & -3169.4 & 1584.7 & 0 \\
0 & 0 & 0 & 2.8H_0 - 1584.7
\end{bmatrix}
\tag{11.18}
$$

The eigenspectrum of (11.18) is plotted as a function of H_0 in Fig. 11.4. The left-hand figure shows all four solutions, and the right-hand the bottom three eigenvalues. The two parallel branches have a constant separation of 6338.7, which is exactly $2J_{exch}$, where J_{exch} is the exchange energy. It is important to note that the transition (resonant) frequency between states 2 and 3 is the same between as between 3 and 4, for all values of H_0: $\omega_{0_{23}} = \omega_{0_{34}}$.

The eigenstates corresponding to the spectrum of Fig. 11.4 are, from the largest to the smallest eigenvalue (in magnitude):

$$
\begin{matrix}
(1) & (2) & (3) & (4)
\end{matrix}
$$

$$
\begin{bmatrix} 0.0 \\ -0.707 \\ +0.707 \\ 0.0 \end{bmatrix}
\begin{bmatrix} 1.0 \\ 0.0 \\ 0.0 \\ 0.0 \end{bmatrix}
\begin{bmatrix} 0.0 \\ 0.707 \\ 0.707 \\ 0 \end{bmatrix}
\begin{bmatrix} 0.0 \\ 0.0 \\ 0.0 \\ 1.0 \end{bmatrix} , \tag{11.19}
$$

where state 1 corresponds to the eigenvalue, 4754.1, in the left-hand part of
Fig. 11.4, and the other eigenvalues are listed in the right-hand part of the figure.

Clearly, state 2 corresponds to both spins being parallel to the static magnetic
field, because this gives the lowest energy level, whereas state 4 corresponds to
both spins being anti-parallel to the field. States 1 and 3 correspond to linear
combinations of spin 1 being parallel and spin 2 anti-parallel, and the converse.
The higher-energy state involves a sum and difference of the parallel-anti-parallel
combination, whereas the lower-energy state involves only the sum of two such
combinations. We'll see this again in the three-electron calculation.

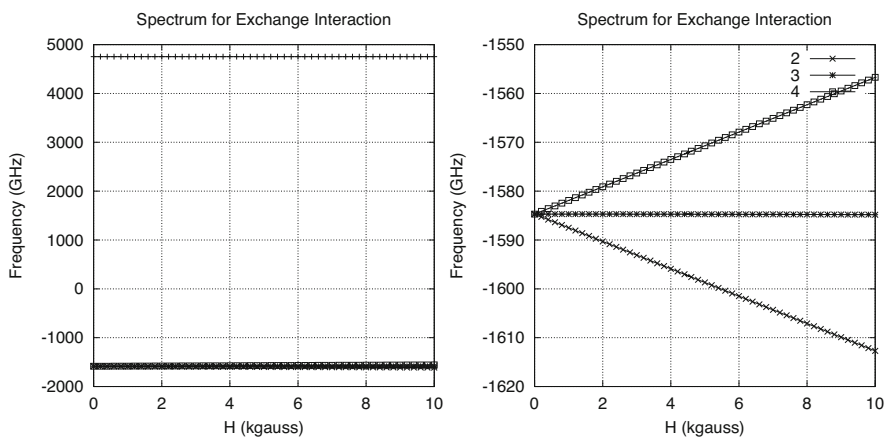The transition matrix elements of the lowest three energy levels are

Fig. 11.4 Eigenspectrum of spin-Hamiltonian with exchange interaction. Left: complete spectrum. Right: expanded version of bottom three eigenvalues

$$\begin{aligned}
S_{x23} &= u_2 \cdot \left(S_x^{(1)} + S_x^{(2)} \right) \cdot u_3 = \quad 0.707 \\
S_{x34} &= u_3 \cdot \left(S_x^{(1)} + S_x^{(2)} \right) \cdot u_4 = \quad 0.707 \\
S_{y23} &= u_2 \cdot \left(S_y^{(1)} + S_y^{(2)} \right) \cdot u_3 = -j0.707 \\
S_{y34} &= u_3 \cdot \left(S_y^{(1)} + S_y^{(2)} \right) \cdot u_4 = -j0.707 \\
S_{z23} &= u_2 \cdot \left(S_z^{(1)} + S_z^{(2)} \right) \cdot u_3 = \quad 0.0 \\
S_{z34} &= u_3 \cdot \left(S_z^{(1)} + S_z^{(2)} \right) \cdot u_4 = \quad 0.0
\end{aligned} \tag{11.20}$$

where the orthonormal eigenvectors, $\{u_i\}$, are given in (11.19), and the spin operators are given in (11.16). These results indicate that one cannot induce transitions by using z-directed AC magnetic fields, as we suspected, and that transitions are equally likely with x- or y-directed AC fields (or with circularly polarized AC fields).

When (11.20) is substituted into the expression, (11.5), for the absorption coefficient and use is made of the fact that $\omega_{0_{23}} = \omega_{0_{34}} = \omega_0$ and $\tau_{23} = \tau_{34} = \tau$, we get, after summing over the bottom three energy-states,

$$A(\omega) = 2 \times \mu_0 \frac{\gamma^2}{4} \frac{1}{Z} \left(e^{-E_2/kT} - e^{-E_4/kT} \right) \frac{\tau/\hbar}{1 + (\omega_0 - \omega)^2 \tau^2} . \tag{11.21}$$

The response is as if the two coupled spins behave as a single spin-system transiting from 'spin-up' (state 2) to 'spin-down' (state 4), which is what we would expect of a two-level (spin-1/2) system.

For comparison, we write down the result for two non-interacting spin-1/2 particles:

$$A(\omega) = 2 \times \mu_0 \frac{\gamma^2}{4} \frac{1}{Z} \left(e^{-E_2/kT} - e^{-E_3/kT} \right) \frac{\tau/\hbar}{1 + (\omega_0 - \omega)^2 \tau^2} . \tag{11.22}$$

Hence, the effect of the exchange interaction is to increase the density of spins in the thermal term by eliminating the middle energy term, $\exp(-E_3/kT)$. Because there is a greater differential in the energies than there was before, we have effectively a greater population difference between the two energy states 2 and 3 that are separated by $\hbar\omega_0$. Clearly, the more interacting spins we have, the greater this population difference becomes, and the greater the absorption spectrum becomes. Because of these two effects, with something of the order of 10^5 spins interacting through the exchange integral, the spectrum becomes significantly larger than in the simple paramagnetic case, giving rise to the name 'superparamagnetism.' We'll give a further example of this next.

Three Spins We'll extend the previous model to include three electrons interacting through the exchange integral. The Hamiltonian now becomes

$$\mathcal{H} = -2.8H_0\left(S_z^{(1)}+S_z^{(2)}+S_z^{(3)}\right) -6338.7\left(\mathbf{S}^{(1)}\cdot\mathbf{S}^{(2)}+\mathbf{S}^{(1)}\cdot\mathbf{S}^{(3)}+\mathbf{S}^{(2)}\cdot\mathbf{S}^{(3)}\right)$$

$$(11.23)$$

where the various three-particle spin-matrices are obtained by taking three-fold left-
and right-direct products of the Pauli spin matrices, $\mathbf{s}$, with the two-dimensional
identity matrix, I_2:

$$\mathbf{S}^{(1)} = \mathbf{s}\otimes I_2\otimes I_2 \quad \mathbf{S}^{(2)} = I_2\otimes\mathbf{s}\otimes I_2 \quad \mathbf{S}^{(3)} = I_2\otimes I_2\otimes\mathbf{s}\ . \tag{11.24}$$

The results are:

$$S_x^{(1)} = \frac{1}{2}\begin{bmatrix} 0_4 & I_4 \\ I_4 & 0_4 \end{bmatrix} \quad S_x^{(2)} = \begin{bmatrix} S_x^{(1)'} & 0_4 \\ 0_4 & S_x^{(1)'} \end{bmatrix} \quad S_x^{(3)} = \begin{bmatrix} S_x^{(2)'} & 0_4 \\ 0_4 & S_x^{(2)'} \end{bmatrix}$$

$$S_y^{(1)} = \frac{1}{2}\begin{bmatrix} 0_4 & -jI_4 \\ jI_4 & 0_4 \end{bmatrix} \quad S_y^{(2)} = \begin{bmatrix} S_y^{(1)'} & 0_4 \\ 0_4 & S_y^{(1)'} \end{bmatrix} \quad S_y^{(3)} = \begin{bmatrix} S_y^{(2)'} & 0_4 \\ 0_4 & S_y^{(2)'} \end{bmatrix} \tag{11.25}$$

$$S_z^{(1)} = \frac{1}{2}\begin{bmatrix} I_4 & 0_4 \\ 0_4 & -I_4 \end{bmatrix} \quad S_z^{(2)} = \begin{bmatrix} S_z^{(1)'} & 0_4 \\ 0_4 & S_z^{(1)'} \end{bmatrix} \quad S_z^{(3)} = \begin{bmatrix} S_z^{(2)'} & 0_4 \\ 0_4 & S_z^{(2)'} \end{bmatrix}$$

where the primed,', submatrices refer to the corresponding 4×4 matrices in (11.16),
and $I_4,\ 0_4$ are the four-dimensional identity and null-matrices, respectively.

Using the results of (11.25), we easily compute the dot-product matrices:

$$\mathbf{S}^{(1)}\cdot\mathbf{S}^{(2)} = \frac{1}{4}\begin{bmatrix} 1 & 0 & 0 & 0 & 0 & 0 & 0 & 0 \\ 0 & 1 & 0 & 0 & 0 & 0 & 0 & 0 \\ 0 & 0 & -1 & 0 & 2 & 0 & 0 & 0 \\ 0 & 0 & 0 & -1 & 0 & 2 & 0 & 0 \\ 0 & 0 & 2 & 0 & -1 & 0 & 0 & 0 \\ 0 & 0 & 0 & 2 & 0 & -1 & 0 & 0 \\ 0 & 0 & 0 & 0 & 0 & 0 & 1 & 0 \\ 0 & 0 & 0 & 0 & 0 & 0 & 0 & 1 \end{bmatrix}$$

$$\mathbf{S}^{(1)}\cdot\mathbf{S}^{(3)} = \frac{1}{4}\begin{bmatrix} 1 & 0 & 0 & 0 & 0 & 0 & 0 & 0 \\ 0 & -1 & 0 & 0 & 2 & 0 & 0 & 0 \\ 0 & 0 & 1 & 0 & 0 & 0 & 0 & 0 \\ 0 & 0 & 0 & -1 & 0 & 0 & 2 & 0 \\ 0 & 2 & 0 & 0 & -1 & 0 & 0 & 0 \\ 0 & 0 & 0 & 0 & 0 & 1 & 0 & 0 \\ 0 & 0 & 0 & 2 & 0 & 0 & -1 & 0 \\ 0 & 0 & 0 & 0 & 0 & 0 & 0 & 1 \end{bmatrix}$$

$$
\mathbf{S}^{(2)} \cdot \mathbf{S}^{(3)} = \frac{1}{4}
\begin{bmatrix}
1 & 0 & 0 & 0 & 0 & 0 & 0 & 0 \\
0 & -1 & 2 & 0 & 0 & 0 & 0 & 0 \\
0 & 2 & -1 & 0 & 0 & 0 & 0 & 0 \\
0 & 0 & 0 & 1 & 0 & 0 & 0 & 0 \\
0 & 0 & 0 & 0 & 1 & 0 & 0 & 0 \\
0 & 0 & 0 & 0 & 0 & -1 & 2 & 0 \\
0 & 0 & 0 & 0 & 0 & 2 & -1 & 0 \\
0 & 0 & 0 & 0 & 0 & 0 & 0 & 1
\end{bmatrix},
\tag{11.26}
$$

from which we get the final expression for the Hamiltonian of (11.23):

$$
\mathscr{H} = -2.8 H_0
\begin{bmatrix}
\frac{3}{2} & & & & & & & \\
 & \frac{1}{2} & & & & & & \\
 & & \frac{1}{2} & & & & & \\
 & & & -\frac{1}{2} & & & & \\
 & & & & \frac{1}{2} & & & \\
 & & & & & -\frac{1}{2} & & \\
 & & & & & & -\frac{1}{2} & \\
 & & & & & & & -\frac{3}{2}
\end{bmatrix}
$$

$$
- \frac{6338.7}{4}
\begin{bmatrix}
3 & 0 & 0 & 0 & 0 & 0 & 0 & 0 \\
0 & -1 & 2 & 0 & 2 & 0 & 0 & 0 \\
0 & 2 & -1 & 0 & 2 & 0 & 0 & 0 \\
0 & 0 & 0 & -1 & 0 & 2 & 2 & 0 \\
0 & 2 & 2 & 0 & -1 & 0 & 0 & 0 \\
0 & 0 & 0 & 2 & 0 & -1 & 2 & 0 \\
0 & 0 & 0 & 2 & 0 & 2 & -1 & 0 \\
0 & 0 & 0 & 0 & 0 & 0 & 0 & 3
\end{bmatrix}.
\tag{11.27}
$$

The diagonal matrix in (11.27) is the projection onto the $z-$axis (the magnetic field) of the combined system of particles. It's eigenvectors are

$$(3/2) \quad (1/2) \quad (1/2) \quad (1/2) \quad (-1/2) \ (-1/2) \ (-1/2) \ (-3/2)$$

$$
\begin{bmatrix} 1.0 \\ 0.0 \\ 0.0 \\ 0.0 \\ 0.0 \\ 0.0 \\ 0.0 \\ 0.0 \end{bmatrix}
\begin{bmatrix} 0.0 \\ 1.0 \\ 0.0 \\ 0.0 \\ 0.0 \\ 0.0 \\ 0.0 \\ 0.0 \end{bmatrix}
\begin{bmatrix} 0.0 \\ 0.0 \\ 1.0 \\ 0.0 \\ 0.0 \\ 0.0 \\ 0.0 \\ 0.0 \end{bmatrix}
\begin{bmatrix} 0.0 \\ 0.0 \\ 0.0 \\ 0.0 \\ 0.0 \\ 0.0 \\ 0.0 \\ 0.0 \end{bmatrix}
\begin{bmatrix} 0.0 \\ 0.0 \\ 0.0 \\ 1.0 \\ 0.0 \\ 0.0 \\ 0.0 \\ 0.0 \end{bmatrix}
\begin{bmatrix} 0.0 \\ 0.0 \\ 0.0 \\ 0.0 \\ 0.0 \\ 1.0 \\ 0.0 \\ 0.0 \end{bmatrix}
\begin{bmatrix} 0.0 \\ 0.0 \\ 0.0 \\ 0.0 \\ 0.0 \\ 0.0 \\ 1.0 \\ 0.0 \end{bmatrix}
\begin{bmatrix} 0.0 \\ 0.0 \\ 0.0 \\ 0.0 \\ 0.0 \\ 0.0 \\ 0.0 \\ 1.0 \end{bmatrix}, \qquad (11.28)
$$

$$(\bullet\,\bullet\,\bullet) \quad (\bullet\,\bullet\,\circ) \quad (\bullet\,\circ\,\bullet) \quad (\circ\,\bullet\,\bullet) \quad (\bullet\,\circ\,\circ) \quad (\circ\,\bullet\,\circ) \quad (\circ\,\circ\,\bullet) \quad (\circ\,\circ\,\circ)$$

where $\bullet$ denotes a spin-up state (parallel to the magnetic field), and $\circ$ denotes a spin-down state.

The eigenspectrum of (11.27), plotted as a function of the static magnetic field, is shown in Fig. 11.5. As is the case with the two-electron problem, the separation between the lowest energy levels is constant and equal to $2.8H_0$ GHz where H_0 is in kGauss. This is identical to the result for a single electron with a spin of 1/2.

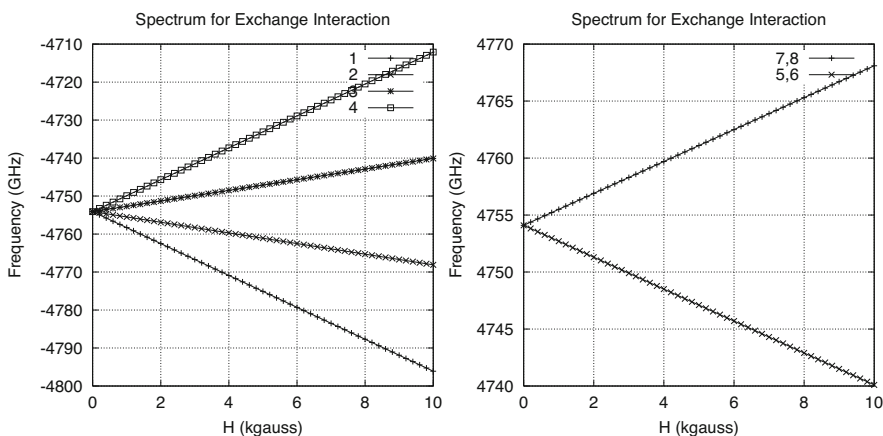The eigenvectors corresponding to the eigenvalues of Fig. 11.5 are:

Fig. 11.5 Eigenspectrum of spin-Hamiltonian with exchange interaction for three electrons. Left: Spectrum of bottom four eigenvalues. Right: Spectrum of two largest (degenerate) eigenvalues. The separation of the average value of each spectral cluster is $9508.2 = 3 \times J_{exch}$ for all H_0

$$
\begin{array}{cccccccc}
(1) & (2) & (3) & (4) & (5) & (6) & (7) & (8)
\end{array}
$$

$$
\begin{bmatrix} 1.0 \\ 0.0 \\ 0.0 \\ 0.0 \\ 0.0 \\ 0.0 \\ 0.0 \\ 0.0 \end{bmatrix}
\begin{bmatrix} 0.0 \\ 0.5774 \\ 0.5774 \\ 0.0 \\ 0.5774 \\ 0.0 \\ 0.0 \\ 0.0 \end{bmatrix}
\begin{bmatrix} 0.0 \\ 0.0 \\ 0.0 \\ 0.5774 \\ 0.0 \\ 0.5774 \\ 0.5774 \\ 0.0 \end{bmatrix}
\begin{bmatrix} 0.0 \\ 0.0 \\ 0.0 \\ 0.0 \\ 0.0 \\ 0.0 \\ 0.0 \\ 1.0 \end{bmatrix}
\begin{bmatrix} 0.0 \\ 0.8165 \\ -0.4082 \\ 0.0 \\ -0.4082 \\ 0.0 \\ 0.0 \\ 0.0 \end{bmatrix}
\begin{bmatrix} 0.0 \\ 0.0 \\ 0.7071 \\ 0.0 \\ -0.7071 \\ 0.0 \\ 0.0 \\ 0.0 \end{bmatrix}
\begin{bmatrix} 0.0 \\ 0.0 \\ 0.0 \\ 0.8165 \\ 0.0 \\ -0.4082 \\ -0.4082 \\ 0.0 \end{bmatrix}
\begin{bmatrix} 0.0 \\ 0.0 \\ 0.0 \\ 0.0 \\ 0.0 \\ 0.7071 \\ -0.7071 \\ 0.0 \end{bmatrix} ,
$$

$$ (11.29) $$

where we note that vectors 5 and 6 correspond to the same eigenvalue, as do 7 and 8.

When we use (11.25) and (11.29), we compute the following transition matrix elements for the lowest four levels:

$$
S_{x_{12}} = 3 \times \frac{0.5774}{2} \quad S_{x_{23}} = 3 \times \frac{0.6667}{2} \quad S_{x_{34}} = 3 \times \frac{0.5774}{2}
$$

$$
S_{y_{12}} = -j3 \times \frac{0.5774}{2} \quad S_{y_{23}} = -j3 \times \frac{0.6667}{2} \quad S_{y_{34}} = -j3 \times \frac{0.5774}{2} \quad (11.30)
$$

$$
S_{z_{12}} = 0 \qquad\qquad S_{z_{23}} = 0 \qquad\qquad S_{z_{34}} = 0
$$

The absorption coefficient for this system is obtained by substituting (11.30) into the general expression, (11.5):

$$
A(\omega) = \frac{\mu_0 \gamma^2}{4Z} \left[3 \left(e^{-E_1/kT} - e^{-E_4/kT} \right) + \left(e^{-E_2/kT} - e^{-E_3/kT} \right) \right] \frac{\tau/\hbar}{1 + (\omega_0 - \omega)^2 \tau^2} .
$$

$$ (11.31) $$

Consider the left-parenthetical term, $3 \left(e^{-E_1/kT} - e^{-E_4/kT} \right) = 3e^{-E_1/kT} \left(1 - e^{-(E_4 - E_1)/kT} \right)$, of (11.31), where $E_4 - E_1 = 3\hbar\omega_0$. Under the usual conditions of room (or body) temperature, and a magnetic field of a few kGauss, the exponent, $(E_4 - E_1)/kT$ is of the order of 10^{-3}, which means that the term in parenthesis is approximately equal to $3 \times \hbar\omega_0/kT$, so that the absorption coefficient in (11.31) is approximately equal to

$$
A(\omega) \approx \frac{9\mu_0 \gamma^2}{4Z} e^{-E_1/kT} \frac{\hbar\omega_0}{kT} \frac{\tau/\hbar}{1 + (\omega_0 - \omega)^2 \tau^2}
$$

$$
= \frac{\mu_0 g^2 h^2 (3\beta)^2}{4Z} \frac{e^{-E_1/kT}}{kT} \frac{\omega_0 \tau}{1 + (\omega_0 - \omega)^2 \tau^2} , \qquad (11.32)
$$

where β is the Bohr magneton (the magnetic dipole of a single spin). Therefore, we can conclude from (11.32) that the exchange interaction causes individual spins to align themselves parallel to each other, thereby producing an atomic system of spin-1/2, but with an equivalent dipole three times that of a single spin-1/2

particle. As indicated in (11.31), the effect of the AC field is to cause this single macrospin system to transit from spin-up to spin-down, with all individual spins remaining parallel to each other. In contrast, three noninteracting spins would have an equivalent absorption coefficient of

$$A(\omega) = \frac{3\mu_0\gamma^2}{4Z}\left(e^{-E_1/kT} - e^{-E_2/kT}\right)\frac{\tau/\hbar}{1 + (\omega_0 - \omega)^2\tau^2}$$

$$\approx \frac{3\mu_0\gamma^2}{4Z}\frac{e^{-E_1/kT}}{kT}\frac{\omega_0\tau}{1 + (\omega_0 - \omega)^2\tau^2} , \qquad (11.33)$$

which is much smaller than (11.32). We can imagine what happens when 10^5 particles interact under exchange effects. This confirms, once again, that the exchange interaction associated with ferromagnetic single-domain particles gives rise to the notion of 'superparamagnetism.'

This model of superparamagnetism results from the large value of J_{exch}, because that isolates the upper energy levels of Figs. 11.4 and 11.5 from the lower levels for all (reasonable) values of H_0. The upper energy levels may be degenerate, as in Fig. 11.5 for the three-spin problem, but the lower levels are always nondegenerate, and have the same number of equal intervals as the number of spins. Furthermore, the large value of the exchange energy ensures that the upper levels will be virtually unpopulated compared to the lower levels. These facts are crucial to the theory.

We can gain further insight into the physics of the problem by considering the combined spin operator $\mathbf{S} = \mathbf{S}^{(1)} + \mathbf{S}^{(2)} + \mathbf{S}^{(3)}$, where the matrices are defined in (11.24) and (11.25). It is straightforward to form $\mathbf{S}^2$, which corresponds to the length-squared of the spin of the composite system of three spin-1/2 particles. The eigenvalues of $\mathbf{S}^2$ give the squares of the lengths when the system is in its allowed states. There are two eigenvalues, 3.750 and 0.750, each four-fold degenerate. Thus, there are two allowed lengths of the composite spin system, $3.750^{1/2}$ and $0.750^{1/2}$. The first corresponds to all three spins being parallel to each other, and the second to two spins being parallel and the third antiparallel. The 'length' of a spin operator is $[S(S + 1)]^{1/2}$, so in the first case $S = 3/2$ and in the second $S = 1/2$. Clearly, the first case corresponds to three spin-1/2 particles being aligned in parallel to each other, and the second to two aligned in parallel and the third oppositely aligned, yielding an effective single spin-1/2 particle.

The eigenvectors of $\mathbf{S}^2$ are precisely those shown in (11.29), with the first four corresponding to the eigenvalue, 3.75, and the last four to the eigenvalue 0.75. In the first case, as we stated above, all spins are aligned with each other, yielding a preferred energy state under the effect of the exchange interaction, whereas the second case corresponds to one particle being oppositely aligned to the other two. This results in a significant energy increase due to the large exchange interaction, and this is exactly what we saw in Fig. 11.5. We can further interpret the left-hand spectrum in Fig. 11.5 as being due to the composite system of three parallel spins oriented so that the net component along the magnetic field is maximum (level 1), 1/2 maximum (level 2), 1/2 maximum, but oriented opposite to the field

(level 3), and maximum orientation opposite to the field (level 4). This supports our earlier conclusion that under the effects of the exchange interaction the three spins behave as a single large moment, as far as the transitions of the lower energies are concerned.

For the two-spin problem, the eigenvalues of $\mathbf{S}^2$ are 2.000, 2.000, 2.000, and 0.000. The eigenvectors corresponding to the first (degenerate) eigenvalue of 2.000 are the second through fourth eigenvectors listed in (11.19), and the eigenvector corresponding to the eigenvalue 0.000 is the first eigenvector listed in (11.19). The interpretation of the two-spin system follows that of the three-spin system; an eigenvalue of 2.000 means that the two spins are parallel to each other in each of the states shown in the right-hand of Fig. 11.4, whereas the zero eigenvalue means that the two spins are oppositely aligned, thereby cancelling each other, resulting in a zero spin, and no energy variation as H_0 is varied in the top curve of the left-hand of Fig. 11.4. The middle curve on the right-hand part of the figure corresponds to the situation in which the 'macrospin' (both spins aligned with each other) is exactly orthogonal to H_0, meaning that there is no energy variation as H_0 is varied. This explains why states 1 and 3 are constant with respect to H_0. Figure 11.6 summarizes the physics of the problem for the two- and three-spin-1/2 systems.

11.4 Fe^{3+} and Hund's Rules

The models that we have considered so far for superparamagnetism comprised two and three independent electrons, coupled through an exchange interaction only. Real systems contain atoms or ions, which comprise collections of electrons, but whose electrons are not independent. We'll give an example of an important ion, triply-ionized iron [97].

The five unpaired electrons in Fe^{3+} are each in the 3d state. This means that the ion itself is in an orbital S state, i.e., $L = 0$, where L is the orbital angular momentum quantum number. To prove this we use Hund's rules together with the Pauli exclusion principle. Hund's rules are:

1. Assign maximum S (spin) consistent with the Pauli principle.
2. Assign maximum L (orbital angular momentum) consistent with the S. L is defined to be the maximum value of the sum of the z-components of orbital angular momentum for the group of electrons.

Thus, each electron has the same energy quantum number, 3, the same orbital angular momentum quantum number, 2 (corresponding to the d-state), and, if we are to assign maximum spin to the electron group, the same spin quantum number, 1/2. If there is to be no violation of the Pauli principle, therefore, each electron must have a different quantum number, m, corresponding to the z-component of orbital angular momentum. Because $l = 2$ for a d-state, we have $m = 2, 1, 0, -1, -2$. Thus, electron number 1 has $m = 2$, number 2 has $m = 1$, etc., to number 5 having $m = -2$. The total $M = m_1 + m_2 + m_3 + m_4 + m_5 = 0$. But since any arrangement
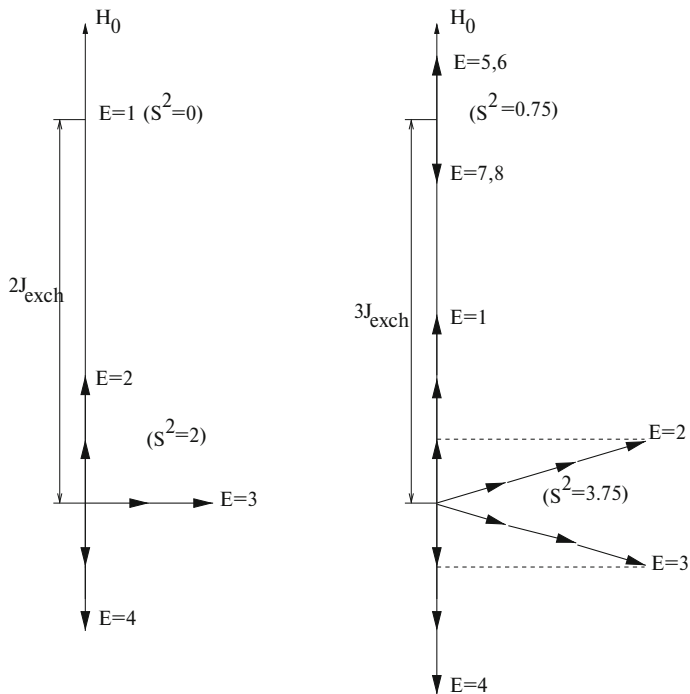
Fig. 11.6 Illustrating the energy levels and states corresponding to two spin-1/2 particles (left) and three spin-1/2 particles (right) in the presence of a magnetic field, H_0. The labeling of the energy eigenstates (E) corresponds to Fig. 11.4 for the two-particle system, and to Fig. 11.5 for the three-particle system. S^2 labels the eigenvalues of the $\mathbf{S}^2$ operator for each of the systems

of the five electrons among the five m-states always yields $M = 0$, we conclude that $L = 0$ (recall that $L = M_{\max}$). Thus, Fe^{3+} is in an S-state ($L = 0$) with a spin equal to 5/2. The fact that $L = 0$ means that the orbital angular momentum is 'quenched,' and cannot contribute to magnetic effects of the ion. Spin is the sole contributor of magnetic effects, and these effects are manifest through the spin-Hamiltonian (Figs. 11.7, 11.8, and 11.9).

The Pauli spin-matrices for a spin-5/2 system are the 6×6 matrices:

$$\sigma_x = \frac{1}{2} \begin{bmatrix} 0 & \sqrt{5} & 0 & 0 & 0 & 0 \\ \sqrt{5} & 0 & \sqrt{8} & 0 & 0 & 0 \\ 0 & \sqrt{8} & 0 & 3 & 0 & 0 \\ 0 & 0 & 3 & 0 & \sqrt{8} & 0 \\ 0 & 0 & 0 & \sqrt{8} & 0 & \sqrt{5} \\ 0 & 0 & 0 & 0 & \sqrt{5} & 0 \end{bmatrix}$$

$$\sigma_y = \frac{1}{2} \begin{bmatrix} 0 & -j\sqrt{5} & 0 & 0 & 0 & 0 \\ j\sqrt{5} & 0 & -j\sqrt{8} & 0 & 0 & 0 \\ 0 & j\sqrt{8} & 0 & -j3 & 0 & 0 \\ 0 & 0 & j3 & 0 & -j\sqrt{8} & 0 \\ 0 & 0 & 0 & j\sqrt{8} & 0 & -j\sqrt{5} \\ 0 & 0 & 0 & 0 & j\sqrt{5} & 0 \end{bmatrix}$$

$$\sigma_z = \frac{1}{2} \begin{bmatrix} 5 & 0 & 0 & 0 & 0 & 0 \\ 0 & 3 & 0 & 0 & 0 & 0 \\ 0 & 0 & 1 & 0 & 0 & 0 \\ 0 & 0 & 0 & -1 & 0 & 0 \\ 0 & 0 & 0 & 0 & -3 & 0 \\ 0 & 0 & 0 & 0 & 0 & -5 \end{bmatrix}. \tag{11.34}$$

The direct-product spin-matrices for the two-ion system are given by $\mathbf{S}^{(1)} = \sigma \otimes I_6$, $\mathbf{S}^{(2)} = I_6 \otimes \sigma$, where I_6 is the six-dimensional identity matrix. Spelled out, these are:

$$S_x^{(1)} = \frac{1}{2} \begin{bmatrix} 0_6 & \sqrt{5}I_6 & 0_6 & 0_6 & 0_6 & 0_6 \\ \sqrt{5}I_6 & 0_6 & \sqrt{8}I_6 & 0_6 & 0_6 & 0_6 \\ 0_6 & \sqrt{8}I_6 & 0_6 & 3 & 0_6 & 0_6 \\ 0_6 & 0_6 & 3 & 0_6 & \sqrt{8}I_6 & 0_6 \\ 0_6 & 0_6 & 0_6 & \sqrt{8}I_6 & 0_6 & \sqrt{5}I_6 \\ 0_6 & 0_6 & 0_6 & 0_6 & \sqrt{5}I_6 & 0_6 \end{bmatrix}$$

$$S_y^{(1)} = \frac{1}{2} \begin{bmatrix} 0_6 & -j\sqrt{5}I_6 & 0_6 & 0_6 & 0_6 & 0_6 \\ j\sqrt{5}I_6 & 0_6 & -j\sqrt{8}I_6 & 0_6 & 0_6 & 0_6 \\ 0_6 & j\sqrt{8}I_6 & 0_6 & -j3I_6 & 0_6 & 0_6 \\ 0_6 & 0_6 & j3I_6 & 0_6 & -j\sqrt{8}I_6 & 0_6 \\ 0_6 & 0_6 & 0_6 & j\sqrt{8}I_6 & 0_6 & -j\sqrt{5}I_6 \\ 0_6 & 0_6 & 0_6 & 0_6 & j\sqrt{5}I_6 & 0_6 \end{bmatrix}$$

$$S_z^{(1)} = \frac{1}{2} \begin{bmatrix} 5I_6 & 0_6 & 0_6 & 0_6 & 0_6 & 0_6 \\ 0_6 & 3I_6 & 0_6 & 0_6 & 0_6 & 0_6 \\ 0_6 & 0_6 & 1I_6 & 0_6 & 0_6 & 0_6 \\ 0_6 & 0_6 & 0_6 & -1I_6 & 0_6 & 0_6 \\ 0_6 & 0_6 & 0_6 & 0_6 & -3I_6 & 0_6 \\ 0_6 & 0_6 & 0_6 & 0_6 & 0_6 & -5I_6 \end{bmatrix}$$

$$S_x^{(2)} = \frac{1}{2} \begin{bmatrix} \sigma_x & 0_6 & 0_6 & 0_6 & 0_6 & 0_6 \\ 0_6 & \sigma_x & 0_6 & 0_6 & 0_6 & 0_6 \\ 0_6 & 0_6 & \sigma_x & 0_6 & 0_6 & 0_6 \\ 0_6 & 0_6 & 0_6 & \sigma_x & 0_6 & 0_6 \\ 0_6 & 0_6 & 0_6 & 0_6 & \sigma_x & 0_6 \\ 0_6 & 0_6 & 0_6 & 0_6 & 0_6 & \sigma_x \end{bmatrix}$$

$$S_y^{(2)} = \frac{1}{2} \begin{bmatrix} \sigma_y & 0_6 & 0_6 & 0_6 & 0_6 & 0_6 \\ 0_6 & \sigma_y & 0_6 & 0_6 & 0_6 & 0_6 \\ 0_6 & 0_6 & \sigma_y & 0_6 & 0_6 & 0_6 \\ 0_6 & 0_6 & 0_6 & \sigma_y & 0_6 & 0_6 \\ 0_6 & 0_6 & 0_6 & 0_6 & \sigma_y & 0_6 \\ 0_6 & 0_6 & 0_6 & 0_6 & 0_6 & \sigma_y \end{bmatrix}$$

$$S_z^{(2)} = \frac{1}{2} \begin{bmatrix} \sigma_z & 0_6 & 0_6 & 0_6 & 0_6 & 0_6 \\ 0_6 & \sigma_z & 0_6 & 0_6 & 0_6 & 0_6 \\ 0_6 & 0_6 & \sigma_z & 0_6 & 0_6 & 0_6 \\ 0_6 & 0_6 & 0_6 & \sigma_z & 0_6 & 0_6 \\ 0_6 & 0_6 & 0_6 & 0_6 & \sigma_z & 0_6 \\ 0_6 & 0_6 & 0_6 & 0_6 & 0_6 & \sigma_z \end{bmatrix} . \tag{11.35}$$

11.5   Crystalline Anisotropy and TiO$_2$

Now we need to include the effects of crystalline anisotropy. The only spin-Hamiltonian that we have for the interaction of a crystal field with Fe^{3+} is for TiO$_2$, and is given in (11.6). When we add the D-term of the crystal field to the spin-Hamiltonian for the Zeeman and exchange interactions, and compute the eigenvalues, we get the results shown in Fig. 11.10 for the lowest eleven frequencies, the 'A-section' of Fig. 11.9. The spectrum of the other five sections of Fig. 11.9 are shown in Figs. 11.11, 11.12, 11.13, 11.14, and 11.15. Clearly, the spectrum is altered significantly by the crystal-field interaction, and that is why this interaction is so important to us. In order for us to 'tune' the system to the proper frequency of operation by adjusting the external magnetic field, we must know the nature of the environment of the iron ion, and how this environment reacts with the ion.

In the example just computed, we see that the lowest energy levels, 1 and 2 in the A-spectrum, have a small separation as H_0 is varied. The frequency interval, ω_{012}, varies between 100 MHz and 1.5 GHz, and the transition-matrix element, S_{y12}, is relatively close to $\pm j4.8$ over this range. This is a considerably larger value of the transition-matrix element than those given in (11.10) for a single, noninteracting spin, and, once again, demonstrates the effect of the exchange interaction.
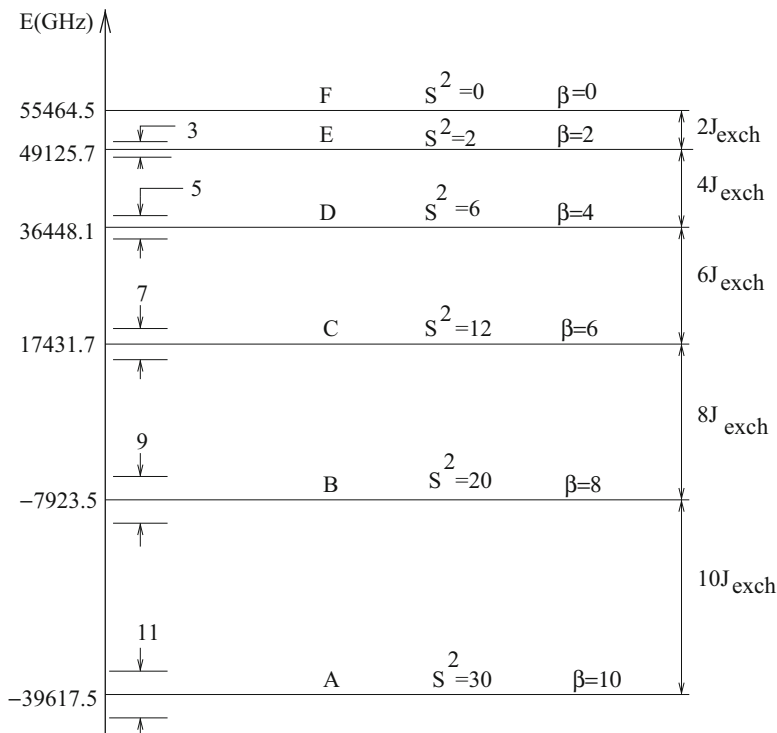
Fig. 11.7 Energy-levels (in GHz) for the system comprising two $Fe^{(3+)}$ ions connected through the exchange interaction J_{exch}. The numbers just inside the vertical line indicate the number of energy levels associated with that branch of the spectrum; the spacing between consecutive pairs of levels is equal to $2.8H_0$, where H_0 is in kGauss. The letters, A-F, correspond to the physical arrangement of the ten electrons in the coupled system, as shown in Table 11.1. S^2 are the eigenvalues of the magnitude-squared spin-operator, $\mathbf{S}^2$, and the β-values indicate the number of Bohr magnetons in the various arrangements of parallel spins

Table 11.1 Spin arrangements for Fig. 11.7. The bullets, •, correspond to spins that are parallel to the $z-$axis, and the circles, ○, to spins that are anti-parallel

A	• • • • • • • • • •	$S = 5 : 2S + 1 = 11$
B	• • • • • • • • • ○	$S = 4 : 2S + 1 = 9$
C	• • • • • • • • ○ ○	$S = 3 : 2S + 1 = 7$
D	• • • • • • • ○ ○ ○	$S = 2 : 2S + 1 = 5$
E	• • • • • • ○ ○ ○ ○	$S = 1 : 2S + 1 = 3$
F	• • • • • ○ ○ ○ ○ ○	$S = 0 : 2S + 1 = 1$

The eigenvalues (in GHz) corresponding to the lowest eleven energy levels (the 'A-section' spectrum of Fig. 11.10) are listed here in the order, E_1 to E_{11}, left-to-right, for $H_0 = 1$ kGauss:

```
h =  1.000000000000000
A-section spectrum
-39662.7967 -39661.1857 -39580.6189 -39558.0700 -39525.8847 -39453.1469
-39436.4784 -39306.8435 -39284.5805 -39098.4235 -39070.4491
```

Fig. 11.8 Positions of the 10-spin magnetic dipole that produce the 'A-spectrum' of Fig. 11.7. The numbering of the energy levels, $E_1 \cdots E_{11}$, corresponds to that of Fig. 11.9
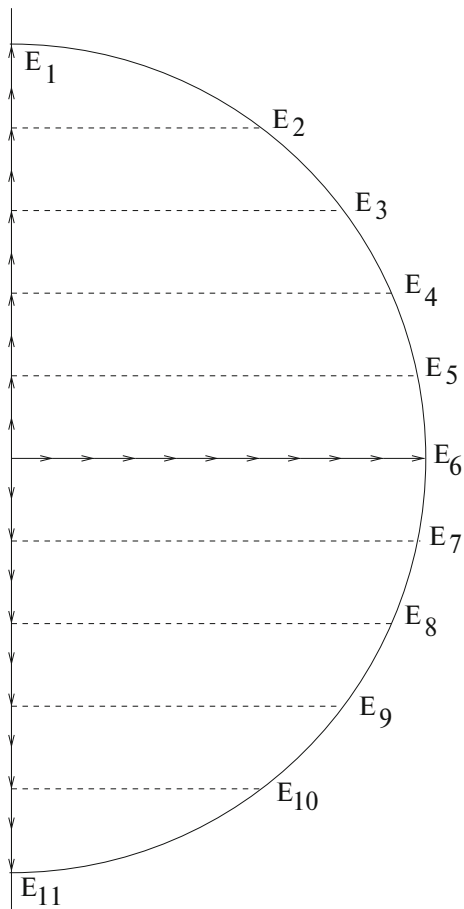
The resonant frequencies (in GHz) associated with transitions between these eigenvalues are:

```
h =  1.000000000000000
A-section resonant frequencies
  1.6109   82.1777 104.7267 136.9120 209.6497 226.3183 355.9532
   378.2162 564.3732 592.3476
 80.5668 103.1157 135.3010 208.0388 224.7073 354.3423 376.6052
  562.7622 590.7366
 22.5489   54.7342 127.4720 144.1405 273.7755 296.0384 482.1954 510.1698
 32.1853 104.9231 121.5916 251.2266 273.4895 459.6465 487.6209
 72.7377   89.4063 219.0412 241.3042 427.4612 455.4356
 16.6685 146.3035 168.5665 354.7234 382.6978
129.6350 151.8979 338.0549 366.0293
 22.2630 208.4200 236.3943
186.1570 214.1314
 27.9744
```

Spectrum for Exchange Interaction
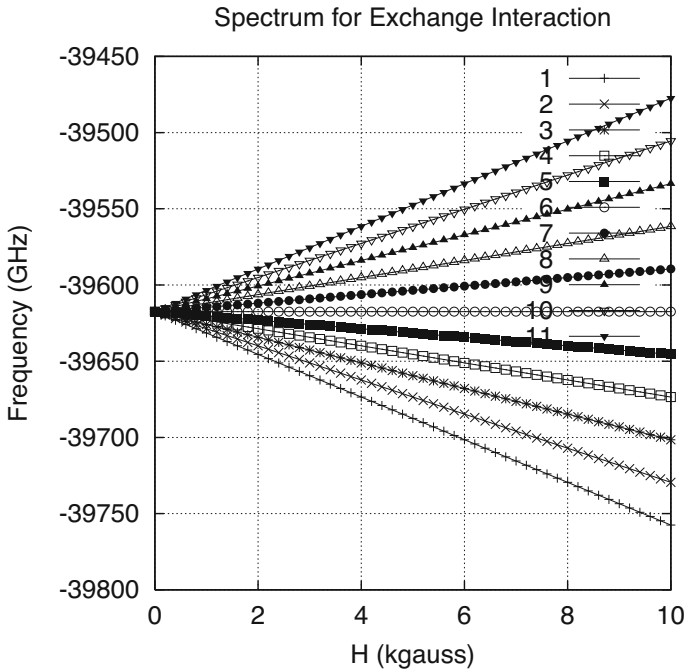
Fig. 11.9 Variation of A-section spectrum of Figs. 11.7 and 11.8 as a function of the magnetic field

The transition-matrix elements, $S_{x_{ij}}$, $S_{y_{ij}}$, $S_{z_{ij}}$, with $i < j$, for the lowest eleven energy levels (the 'A-spectrum') are shown next for $H_0 = 1$ kGauss. The $S_{y_{ij}}$ are complex–in this case pure imaginaries.

```
h =  1.000000000000000
transx
0.0340 2.3641  0.0000 0.0000 -0.3188 -0.3458 0.0000 0.0000 0.0104 0.0083
0.0000 2.2114 -0.2267 0.0000  0.0000 -0.0881 0.0708 0.0000 0.0000
0.4898 3.4479  0.0000 0.0000 -0.2023 -0.1794 0.0000 0.0000
0.0000 2.3182 -1.2585 0.0000  0.0000 -0.0475 0.0315
1.5273 2.5256  0.0000 0.0000 -0.0396 -0.0480
0.0000 2.3001 -0.2578 0.0000  0.0000
0.2658 2.2929  0.0000 0.0000
0.0000 1.6855 -0.0044
0.0044 1.6823
0.0000
transy
0.0000  4.8024 0.0000 -0.0927 0.0000 0.0000 0.0000 0.0000 0.0000 -0.3642
0.0000  0.2450 0.0000  0.0000 0.0000 0.0000 0.0000 0.0096 0.0000 -0.0077
0.0000  0.0000 0.0000  0.1411 0.0000 0.8497 0.0000 0.0000 0.0000  0.0000
0.0000 -0.0777 0.0000 -0.0633 0.0000 0.0000 0.0000 0.0000
0.0000  3.2101 0.0000 -0.5124 0.0000 0.0000 0.0000 0.0000 0.0000 -0.1786
0.0000  0.1571 0.0000  0.0000 0.0000 0.0000
0.0000  0.0000 0.0000  1.3829 0.0000 1.2520 0.0000 0.0000 0.0000  0.0000
0.0000 -0.0435 0.0000 -0.0289
```
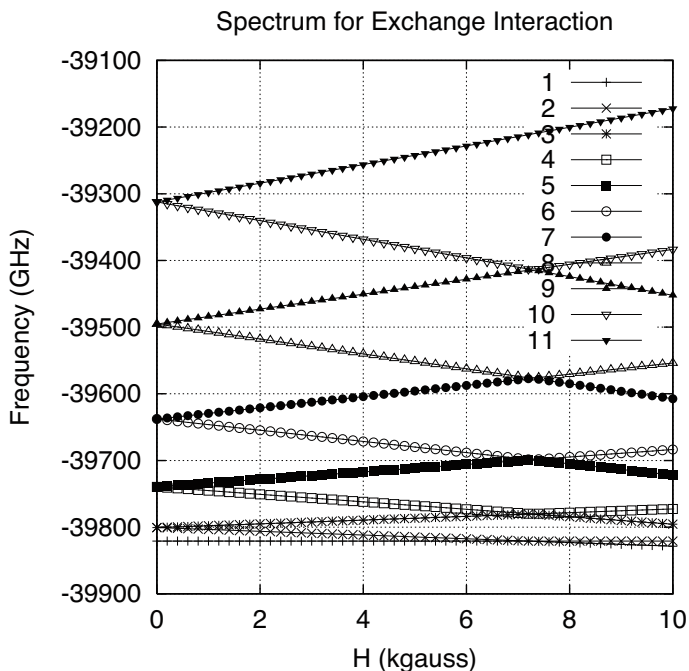
Fig. 11.10 Modification of the A-section spectrum of Fig. 11.9 due to the *D*-term of the crystal field spin-Hamiltonian of TiO$_2$ shown in (11.6)

```
0.0000  1.5732 0.0000 -1.6175 0.0000 0.0000 0.0000 0.0000 0.0000 -0.0360
0.0000  0.0438
0.0000  0.0000 0.0000  1.9029 0.0000 0.2246 0.0000 0.0000 0.0000  0.0000
0.0000  0.2310 0.0000 -1.9156 0.0000 0.0000 0.0000 0.0000
0.0000  0.0000 0.0000  1.4797 0.0000 0.0039
0.0000  0.0039 0.0000 -1.4829
0.0000  0.0000
transz
0.0000 0.0000 -0.9531  0.1054  0.0000 0.0000 0.0335 -0.0271 0.0000 0.0000
1.0827 0.0000  0.0000 -0.1526 -0.1637 0.0000 0.0000  0.0038 0.0030
0.0000 0.0000 -0.5122  0.3721  0.0000 0.0000 0.0089 -0.0076
1.7013 0.0000  0.0000 -0.1711 -0.1161 0.0000 0.0000
0.0000 0.0000 -0.1487  0.1827  0.0000 0.0000
0.6668 0.0000  0.0000 -0.0964 -0.0108
0.0000 0.0000 -0.0114  0.0935
0.0208 0.0000  0.0000
0.0000 0.0000
0.0002
```

Let's use these results to calculate the peak value of the absorption coefficient for those transitions that occur with a frequency less than 50 GHz. According to the table of 'A-section resonant frequencies,' there are six such transitions: 12, 34, 45, 67, 89, 1011. According to (11.5), the peak value of the absorption coefficient is given by
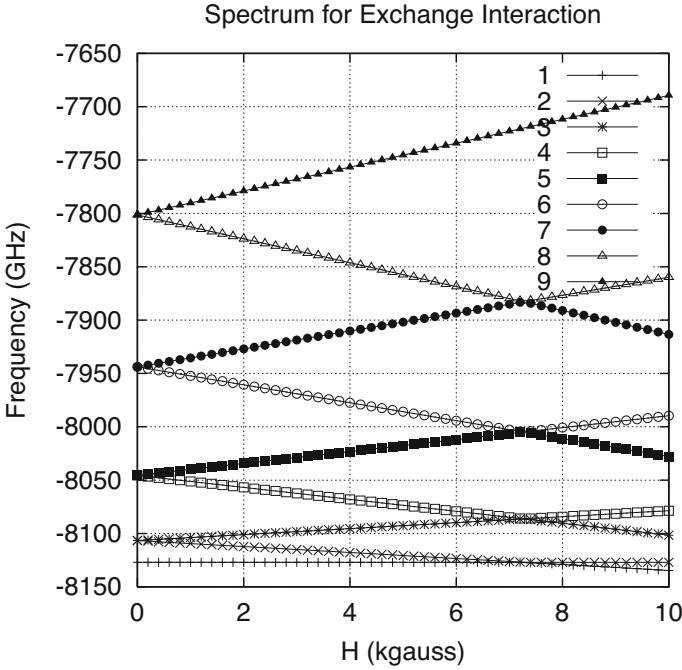
Fig. 11.11 Modification of the B-section spectrum of Fig. 11.9 due to the D-term of the crystal field spin-Hamiltonian of TiO_2 shown in (11.6)

$$A(\omega_{0_{jk}}) \propto |S_{kj}|^2 \left(N_j^{(T)} - N_k^{(T)} \right) \tau_{jk}/\hbar$$

$$= |S_{kj}|^2 N_j \left(1 - e^{-(E_k - E_j)/kT} \right) \tau_{jk}/\hbar$$

$$\approx |S_{kj}|^2 N_j \frac{(E_k - E_j)}{kT} \frac{\tau_{jk}}{\hbar}$$

$$= |S_{kj}|^2 N_j \frac{\hbar\omega_{0_{jk}}}{kT} \frac{\tau_{jk}}{\hbar}$$

$$= |S_{kj}|^2 N_j \frac{\omega_{0_{jk}} \tau_{jk}}{kT} \ . \tag{11.36}$$

We will assume that the temperature is 98.6 °F, which is 310 °K, so that $kT = 4.2811 \times 10^{-21}$ J. To express this in terms of frequency, divide by Planck's constant, 6.626×10^{-34} J, and get 6.461×10^{12} Hz $= 6461.1$ GHz. Since this number is much greater than the resonant frequencies, we are permitted to carry out the approximation in the third line of (11.36). The transition matrix elements in (11.36) include S_x, S_y, and S_z (transx, transy, transz, respectively), and from here on we will assume that the relaxation frequency, τ_{jk}, is fixed for all transitions.
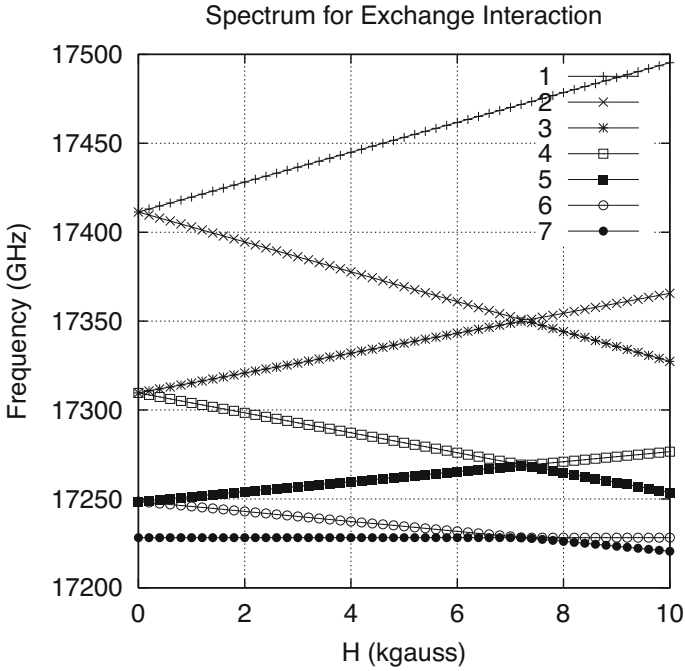
Spectrum for Exchange Interaction

Fig. 11.12 Modification of the C-section spectrum of Fig. 11.9 due to the *D*-term of the crystal field spin-Hamiltonian of TiO$_2$ shown in (11.6)

The following table lists important data for the calculations:

Transition	ω_{0j} (GHz)	Transx	Transy	Transz	N_j/N_1	ω_{0j}/ω_{01}
12	1.6109	0.0340	j4.8024	0.0	1	1
34	22.5489	0.4898	j3.2101	0.0	0.987	14.0
45	32.1853	0.0	0.0	1.7013	0.984	19.98
67	16.6685	0.0	0.0	0.6668	0.968	10.35
89	22.2630	0.0	0.0	0.0208	0.946	13.82
10,11	27.9744	0.0	0.0	0.0002	0.916	17.37

It turns out that the first three absorption lines are much stronger than the others, and these are plotted in Fig. 11.16. This is an example of how we can 'tune' our system to achieve a design feature once we have the physics in the form of a mathematical model. Even though the two higher-frequency lines are stronger, practical considerations would lead us to use the response at 1.6109 GHz for noninvasive probing for lesions.
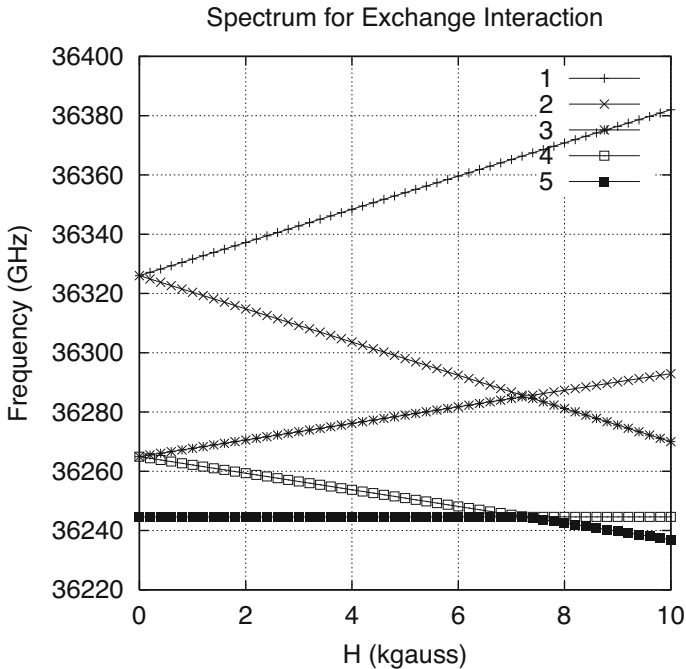
Fig. 11.13 Modification of the D-section spectrum of Fig. 11.9 due to the *D*-term of the crystal field spin-Hamiltonian of TiO_2 shown in (11.6)

11.5.1 Application to a 'Magnetic Lesion'

Consider the model shown in Fig. 11.17, which corresponds to Fig. 10.8, except that the background is tissue with a conductivity that is the average of that found in the body, and the lesion is nonconducting, but is magnetically permeable. If we assume that the same coil is used as in the model of Fig. 10.8, and that the lesion is much deeper, being 5 cm beneath the surface, and that the coil is excited at 1.6 GHz, which corresponds to the lowest transition frequency described above, then the response of the probe to the lesion, whose permeability (at 1.6 GHz) is $\mu = 2, \ 10, \ $ and 100, is shown in Fig. 11.18.

11.6 Static Interaction Energy of Two Magnetic Moments

The spin-Hamiltonian that we have worked with so far includes only the Zeeman term and the exchange interaction. There are other terms that reflect certain physical processes that need to be included, as well. One such term corresponds to the static interaction energy of two magnetic moments [72, p. 412]: $H' =$
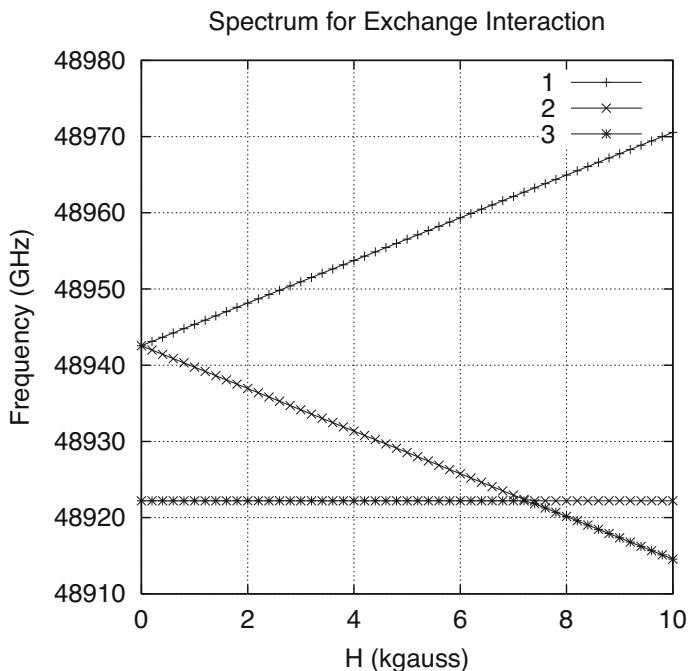
Fig. 11.14 Modification of the E-section spectrum of Fig. 11.9 due to the D-term of the crystal field spin-Hamiltonian of TiO_2 shown in (11.6)

$\frac{\mu_0}{4\pi r^3}\left[\mathbf{m}_1 \cdot \mathbf{m}_2 - 3\frac{(\mathbf{m}_1 \cdot \mathbf{r})(\mathbf{m}_2 \cdot \mathbf{r})}{r^2}\right]$, where $\mathbf{m}_1$ and $\mathbf{m}_2$ are the magnetic moments of the dipoles, and $\mathbf{r}$ is the vector separation between the two dipoles. This energy term manifests itself in the following spin-Hamiltonian for three interacting electrons:

$$\mathscr{H}_{dd} = \frac{\mu_0}{4\pi}4\beta_0^2\left[\frac{\mathbf{S}_1 \cdot \mathbf{S}_2}{r_{12}^3} + \frac{\mathbf{S}_1 \cdot \mathbf{S}_3}{r_{13}^3} + \frac{\mathbf{S}_2 \cdot \mathbf{S}_3}{r_{23}^3}\right.$$

$$\left.-3\frac{(\mathbf{r}_{12} \cdot \mathbf{S}_1)(\mathbf{r}_{12} \cdot \mathbf{S}_2)}{r_{12}^5} - 3\frac{(\mathbf{r}_{13} \cdot \mathbf{S}_1)(\mathbf{r}_{13} \cdot \mathbf{S}_3)}{r_{13}^5} - 3\frac{(\mathbf{r}_{23} \cdot \mathbf{S}_2)(\mathbf{r}_{23} \cdot \mathbf{S}_3)}{r_{23}^5}\right], (11.37)$$

where $\beta_0 = 9.2731 \times 10^{-24}$ amp $-$ meters^2 is the Bohr magneton, and the various vector spin-matrices have been defined earlier. If we assume that the spins lie at the vertices of an equilateral triangle of side 6×10^{-10}m, as in Fig. 11.19, then we can expand (11.37) to get

$$\mathscr{H}_{dd} = 0.24\left[\mathbf{S}_1 \cdot \mathbf{S}_2 + \mathbf{S}_1 \cdot \mathbf{S}_3 + \mathbf{S}_2 \cdot \mathbf{S}_3 - 3S_x^{(1)}S_x^{(2)} - 0.75\left(S_x^{(1)}S_x^{(3)} + S_x^{(2)}S_x^{(3)}\right)\right.$$
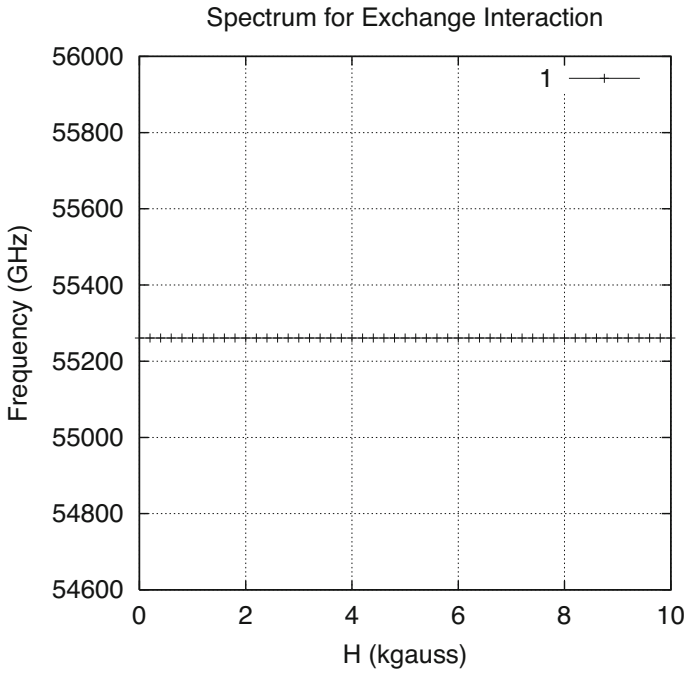
Fig. 11.15 Modification of the F-section spectrum of Fig. 11.9 due to the *D*-term of the crystal field spin-Hamiltonian of TiO$_2$ shown in (11.6)
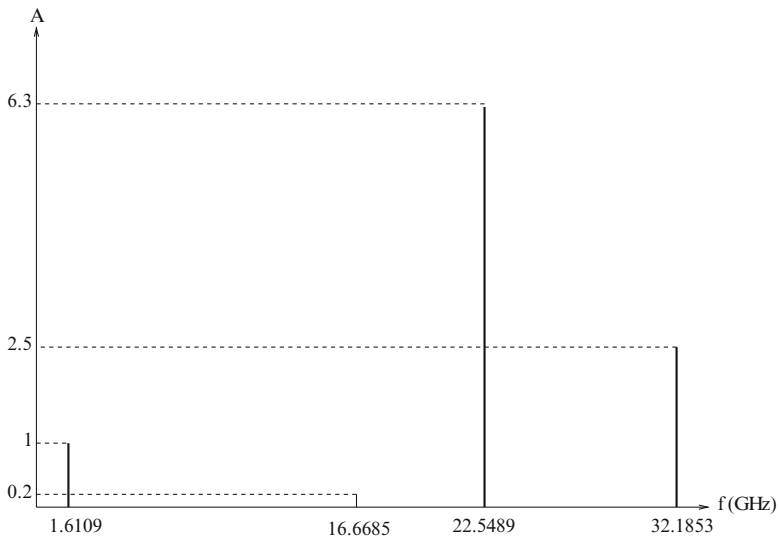

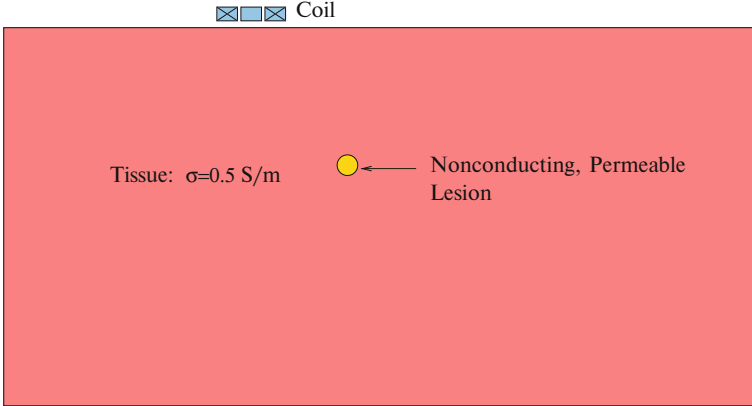**Fig. 11.16** Relative absorption peaks versus frequency

Fig. 11.17 Model of an eddy-current probe scanned past a nonconducting, magnetically permeable lesion embedded in tissue of an averaged conductivity
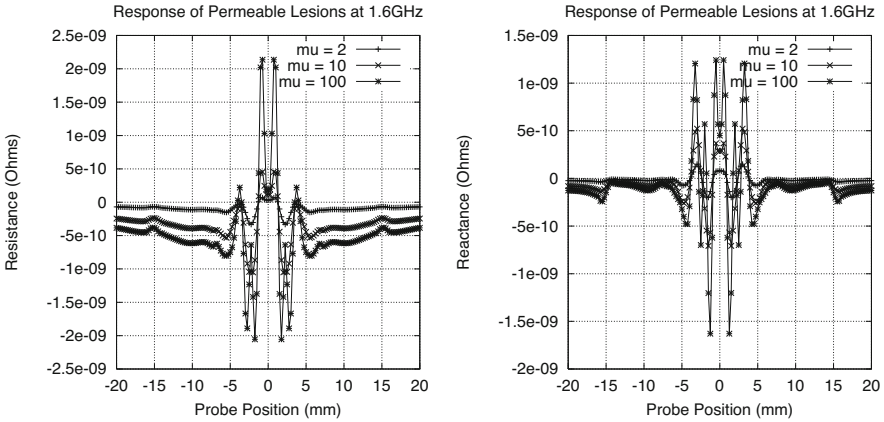

Fig. 11.18 Response of probe to a lesion whose permeability (at 1.6 GHz) is $\mu = 2,\ 10,\ $ and 100

$$+1.299 \left(S_y^{(1)} S_x^{(3)} + S_x^{(1)} S_y^{(3)} - S_y^{(2)} S_x^{(3)} - S_x^{(2)} S_y^{(3)} \right)$$

$$-2.25 \left(S_y^{(1)} S_y^{(3)} + S_y^{(2)} S_y^{(3)} \right) \Big] ,$$

$$(11.38)$$

where the units of $\mathscr{H}_{dd}$ in (11.38) are in GHz. This matrix operator is added to that in (11.27) to get the overall spin-Hamiltonian for Zeeman + Exchange + Dipolar effects.

Fig. 11.19 Illustrating three
magnetic dipoles, labeled as
spin operators, **S**, situated on
the vertices of an equilateral
triangle, for the purpose of
computing the dipole-dipole
interaction